Climatic controls on individual ostracode stable isotopes in a desert lake: a modern baseline for Lake Turkana
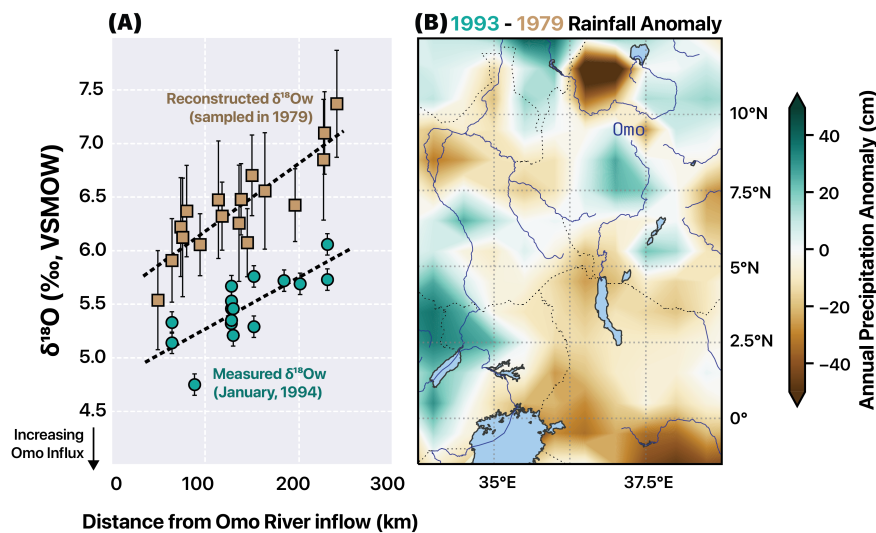
Kaustubh Thirumalai[1,1], Andrew S Cohen[1,1], and Dustin Taylor[1,1]
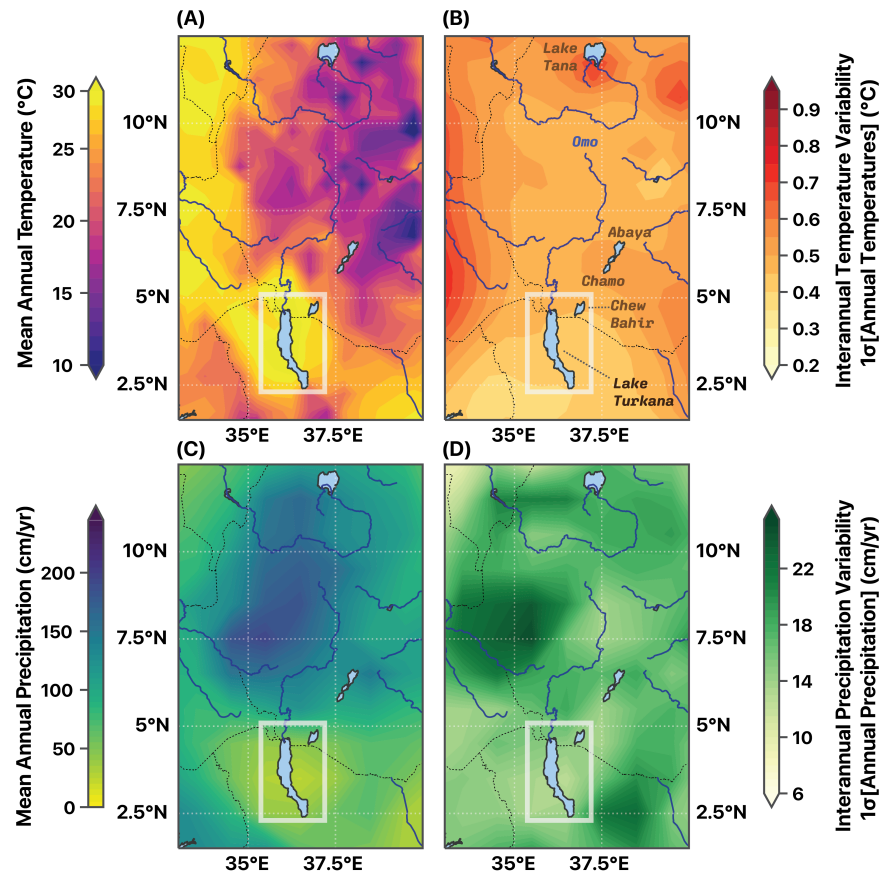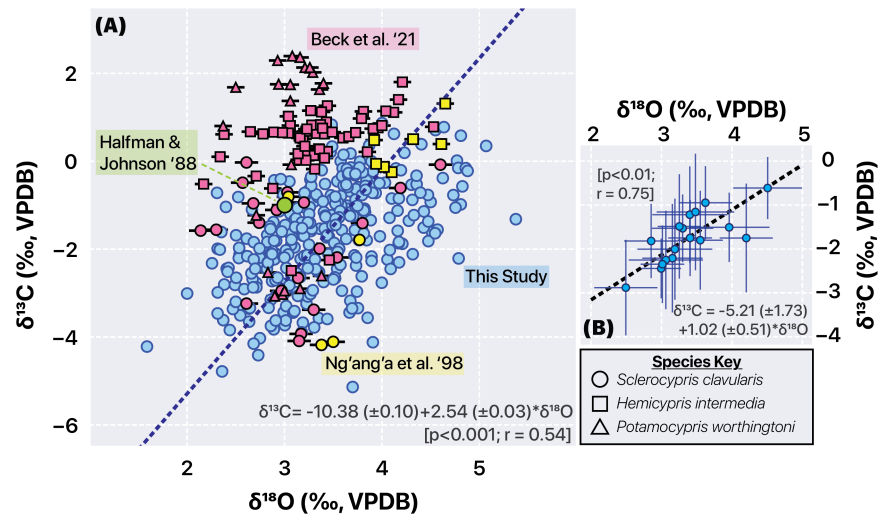
[1]University of Arizona

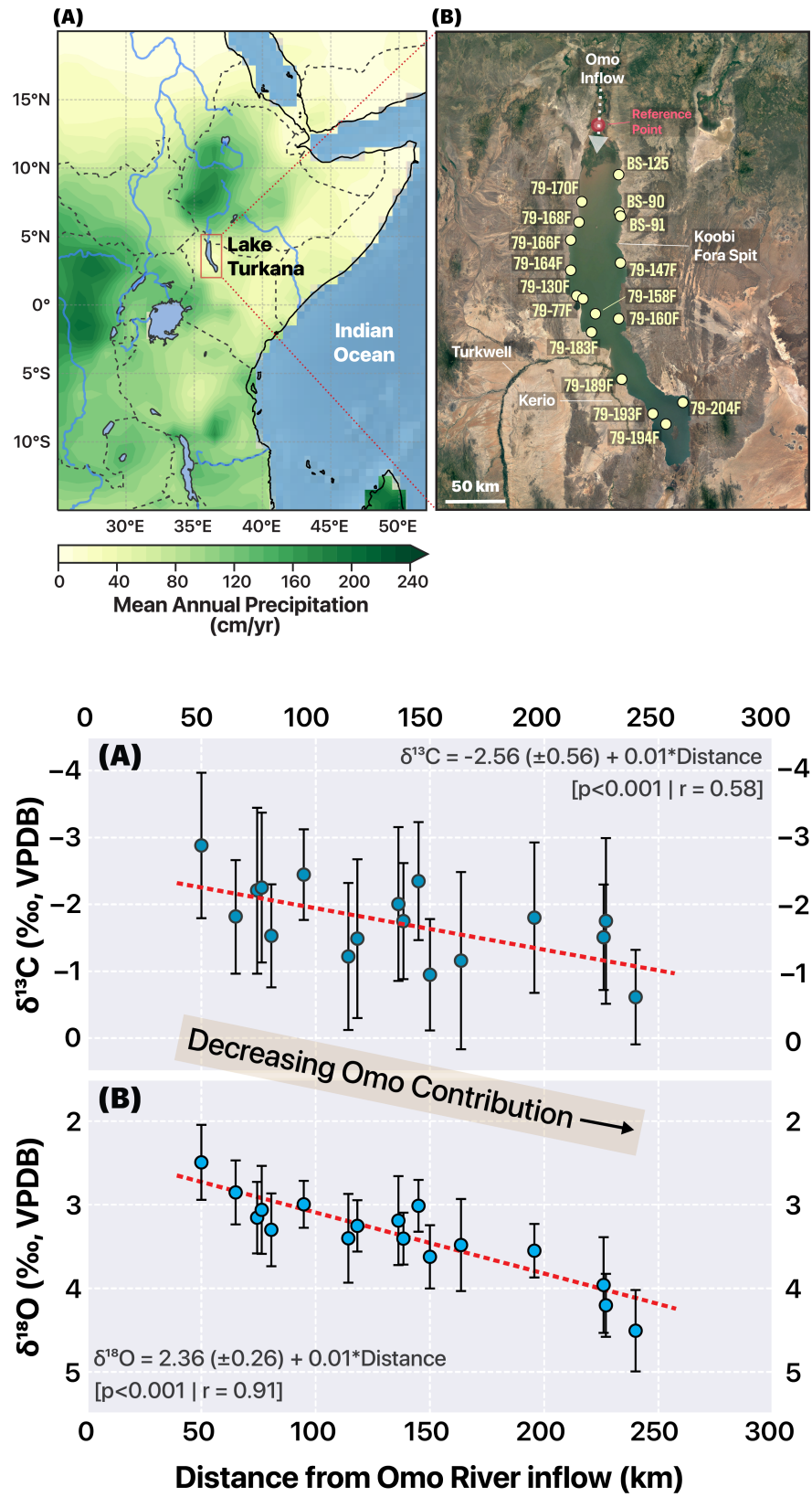December 7, 2022

Abstract

Stable carbon (δ^{13}C) and oxygen (δ^{18}O) isotope measurements in lacustrine ostracodes are widely used to infer past climatic conditions. Previous work has used individual ostracode valves to resolve seasonal and subdecadal climate signals, yet environmental controls on geochemical variability within co-occurring specimens from modern samples are poorly constrained. Here we focus on individual ostracode valves in modern-aged Lake Turkana sediments, an alkaline desert lake in tropical East Africa. We present individual ostracode valve analyses (IOVA) of δ^{13}C and δ^{18}O measurements (n = 329) of extant species Sclerocypris clavularis from 17 sites spanning the entire lake (n-avg ~19 specimens per site). We demonstrate that the pooled statistics of individual valve measurements at each site overcome inter-specimen isotopic variance and are driven by hydrological variability in the lake. Mean IOVA-δ^{13}C and -δ^{18}O across the sites exhibit strong spatial trends with higher values at more southerly latitudes, modulated by distance from the inflow of the Omo River. Whereas the latitudinal δ^{13}C gradient reflects low riverine δ^{13}C and decreasing lacustrine productivity towards the southern part of the lake, the δ^{18}O gradient is controlled by evaporation superimposed on the waning influence of low-δ^{18}O Omo River waters, sourced from the Ethiopian highlands. We show that ostracode δ^{18}O proximal to Omo River inflow is deposited under near-equilibrium conditions and that inter-specimen δ^{18}O variability across the basin is consistent with observed temperature and lake water δ^{18}O variability. IOVA can provide skillful constraints on high-frequency paleoenvironmental signals and, in Omo-Turkana sediments, yield quantitative insights into East African paleohydrology.

1

$\delta^{13}C = -10.38\ (\pm 0.10) + 2.54\ (\pm 0.03)*\delta^{18}O$
[p<0.001; r = 0.54]

$\delta^{13}C = -5.21\ (\pm 1.73)$
$+1.02\ (\pm 0.51)*\delta^{18}O$
[p<0.01; r = 0.75]

1
2

Climatic controls on individual ostracode stable isotopes in a desert lake: a modern baseline for Lake Turkana

3

K. Thirumalai[1], A. S. Cohen[1], D. Taylor[1]

4
5

[1] Department of Geosciences, University of Arizona, 1040 E. 4th Street Tucson, AZ 85721 United States of America

6

Corresponding author: Kaustubh Thirumalai (kaustubh@arizona.edu)

7

Key Points:

8
9

- We present a calibration of individual ostracode valve analyses (IOVA) of $\delta^{18}O$ and $\delta^{13}C$ of *S. clavularis* in modern Lake Turkana sediments.

10
11

- We find that Omo River inflow controls the pooled statistics of IOVA $\delta^{18}O$ and $\delta^{13}C$ across sites.

12
13

- $\delta^{18}O$ values of *S. clavularis* are consistent with effective calcite precipitation under near-equilibrium conditions.

14

15 **Abstract**

16 Stable carbon ($\delta^{13}C$) and oxygen ($\delta^{18}O$) isotope measurements in lacustrine ostracodes are widely
17 used to infer past climatic and paleolimnological conditions. Previous work has used individual
18 ostracode valves to resolve seasonal and subdecadal climate signals, yet environmental controls
19 on geochemical variability within co-occurring specimens from modern samples are poorly
20 constrained. Here we focus on individual ostracode valves in modern-aged Lake Turkana
21 sediments, an alkaline desert lake in tropical East Africa. We present individual ostracode valve
22 analyses (IOVA) of $\delta^{13}C$ and $\delta^{18}O$ measurements (n = 329) of extant species *Sclerocypris*
23 *clavularis* from 17 sites spanning the entire lake (n_{avg} = ~19 specimens per site). We demonstrate
24 that the pooled statistics of individual valve measurements at each site overcome inter-specimen
25 isotopic variance and are driven by hydrological variability in the lake. Mean IOVA-$\delta^{13}C$ and -
26 $\delta^{18}O$ across the sites exhibit strong spatial trends with higher values at more southerly latitudes,
27 modulated by distance from the inflow of the Omo River. Whereas the latitudinal $\delta^{13}C$ gradient
28 reflects low riverine $\delta^{13}C$ and decreasing lacustrine productivity towards the southern part of the
29 lake, the $\delta^{18}O$ gradient is controlled by evaporation superimposed on the waning influence of
30 low-$\delta^{18}O$ Omo River waters, sourced from the Ethiopian highlands. We show that ostracode $\delta^{18}O$
31 proximal to Omo River inflow is deposited under near-equilibrium conditions and that inter-
32 specimen $\delta^{18}O$ variability across the basin is consistent with observed temperature and lake water
33 $\delta^{18}O$ variability. IOVA can provide skillful constraints on high-frequency paleoenvironmental
34 signals, and in Omo-Turkana sediments, yield quantitative insights into East African
35 paleohydrology.

36

37 **Plain Language Summary**

38 Ostracodes are microscopic, aquatic crustaceans that deposit shells ('valves') made of
39 calcium carbonate. Retrieved from sediment cores, these valves are widely used to estimate past
40 water conditions using their shell chemistry. Here we focus on stable oxygen and carbon isotopes
41 in numerous, individual valves in modern sediments taken from multiple sites across Lake
42 Turkana, Kenya. This lake is located in a hot and arid region in equatorial East Africa. The major
43 river that drains into Lake Turkana is the Omo River, which is sourced from rainfall in the
44 Ethiopian Highlands. We find that ostracode stable isotopes are excellent recorders of lake
45 hydrology in this basin and reveal a strong influence of the influx of Omo River waters.
46 Analyzing several valves at each site helps overcome non-environmental controls on ostracode
47 stable isotopes and allows for more accurate estimates of past water conditions. Our results
48 provide a modern baseline of ostracode stable isotopes at Lake Turkana. We suggest that both
49 the average of, and variations within individual-valve measurements of ostracode geochemistry
50 can help characterize past hydrological variability and lake water conditions.

51 **1. Introduction**

52 The geochemistry of lacustrine ostracode shells has provided key insights into continental
53 paleoclimatic fluctuations across the Phanerozoic eon. Stable carbon ($\delta^{13}C$) and oxygen ($\delta^{18}O$)
54 analyses[†] of calcareous ostracode valves found in lake sediments have been used to reconstruct

---

[†] Stable isotopes in this work are reported using the standard δ notation: $\delta_x = \left(\frac{R_x}{R_{std}} - 1\right) \times 1000$, where R is the
ratio of the abundance of the rare versus abundant isotope, x is the sample, and *std* is a reference standard. Here,

55 mean variations in past productivity, temperature, riverine inflow, and chemical composition of
56 lake waters, as well as their links with regional hydroclimate change (Last et al., 1994; Palacios-
57 Fest et al., 1994; Dixit et al., 2014; Pérez et al., 2013; Dettman et al., 1995; Dettman et al., 2005).

58   Conventionally, several ostracode valves from the same sedimentary interval are
59 combined to generate a single measurement ("multi-specimen analysis"), whose value is thought
60 to reflect the average ostracode isotopic composition across the timespan represented by that
61 sample (Dixit et al., 2015; Escobar et al., 2010). However, it is well-known that ostracode
62 calcification occurs rapidly, on the order of hours to days (Turpen & Angell, 1971; Chivas et al.,
63 1986; Roca & Wansard, 1997) – timescales much smaller than the seasonal to centennial
64 duration encompassed in a typical lacustrine time-averaged sample (Holmes, 2008). Multiple
65 studies have investigated sample-size limitations associated with this approach, either through
66 replicate multi-specimen analyses or via numerous measurements of individual ostracode valves
67 ("individual ostracode valve analyses", abbreviated hereafter as IOVA) and have uncovered
68 substantial geochemical variance amongst co-occurring specimens (Dixit et al., 2015; Palacios-
69 Fest & Dettman, 2001; Holmes et al., 1995; Von Grafenstein et al., 1999; Schwalb et al., 2002;
70 Heaton et al., 1995; Holmes, 2008). Citing both non-equilibrium effects as well as the short-lived
71 duration of ostracode calcification relative to sample resolution, these findings called for the
72 combination of large numbers of individual valves (n>15) in multi-specimen measurements to
73 robustly reconstruct mean environmental conditions within a stratigraphic interval (Xia et al.,
74 1997; Palacios-Fest & Dettman, 2001; Holmes, 2008; Escobar et al., 2010; Dixit et al., 2015).

75   On the other hand, few studies have taken advantage of the potential for rapidly deposited
76 ostracode calcite to sample higher frequency subdecadal signals such as seasonality or
77 interannual variability of lake temperature and hydrology. Notably, Dettman et al. (1995)
78 measured individual-valve stable isotopes of various early- to mid-Holocene ostracode species in
79 Lake Huron sediments to identify cold-season $\delta^{18}O$ extremes within sampled intervals. Escobar
80 et al. (2010) applied individual ostracode-valve analyses of $\delta^{18}O$ (IOVA-$\delta^{18}O$) in *Cytheridella*
81 *ilosvayi* specimens from lake sediments of the Yucatán Peninsula to constrain subdecadal
82 hydrological variability across various late Holocene periods. More recently, Dixit et al. (2015)
83 measured individual *Cyprideis torosa* valves in early Holocene intervals of paleolake Riwasa
84 sediments in northern India and suggested that IOVA-$\delta^{18}O$ variance resulted from seasonal
85 temperature and monsoon-driven hydroclimatic fluctuations. Collectively, these studies found
86 intervals of large IOVA-$\delta^{18}O$ variance (interpreted to be environmentally mediated), ranging
87 from ~5-15 ‰. Yet, to our knowledge, no study has conducted a systematic modern calibration
88 between IOVA-$\delta^{18}O$ and observed lake conditions to investigate the fidelity of this approach in
89 reconstructing high-frequency climate variability.

90   In this work, we report IOVA-$\delta^{18}O$ and -$\delta^{13}C$ in *Sclerocypris clavularis,* a relatively
91 large, benthic ostracode that occurs commonly throughout Lake Turkana (Cohen, 1986). Our
92 specimens from modern Lake Turkana sediments were collected from 17 different sites around
93 the lake (Fig. 1B). Our main aims are to 1) characterize within-site isotopic variance across our
94 individual measurements and compare pooled IOVA statistics across the basin, 2) investigate
95 oxygen isotope equilibrium in ostracode calcite at Lake Turkana, 3) provide a modern stable
96 isotope baseline at Lake Turkana as a benchmark for future studies utilizing IOVA, and 4)

---

values are reported in permil (‰) relative to the Vienna Pee Dee Belemnite (VPDB) reference for $\delta^{18}O$ and $\delta^{13}C$,
whereas $\delta^{18}O$ of waters are reported relative to Vienna Standard Mean Oceanic Water (VSMOW).

97 explore the potential of this tool for inferring past hydrologic conditions within the lake and its
98 watershed.

2. Climatic and Hydrological Setting

100 Lake Turkana, one of the great East African Rift Valley lakes, is a closed-basin system
101 (*i.e.,* no direct outflow) situated in an arid region of equatorial eastern Africa. On average, the
102 region receives less than ~25 cm of rainfall per year (Fig. 1). In contrast, the Ethiopian
103 highlands located to the north, are much wetter, with upwards of 150 cm of average rainfall per
104 year (Fig. 2C). Sourced in these highlands, the perennial Omo River comprises the major (>80-
105 90 %) riverine inflow for Lake Turkana, with the Kerio and Turkwell rivers on the southern side
106 being minor contributors (Avery & Tebbs, 2018) (Fig. 1). Mean annual air temperatures in the
107 region are ~29-30 °C (Fig. 2A) and mean annual lake water temperatures are on average, cooler
108 by 1-2 °C (Harbott et al., 1982), although, lake temperatures may ephemerally rise in some
109 months to as high as ~30-31 °C (Källqvist et al., 1988). There is a modest north-south
110 temperature gradient, with surface waters being on average ~1 °C cooler (Harbott et al., 1982)
111 towards the southern end of the lake (which is also deeper). The water column across the lake is
112 generally well-mixed, although a seasonal thermocline and partial stratification may occur during
113 certain times of the year (Källqvist et al., 1988).

114 Compared to adjacent regions, year-to-year variability in temperature and precipitation in
115 Lake Turkana is relatively muted (Fig. 2). Interannual (year-to-year) variability, defined here as
116 one standard deviation (1σ) of annual mean air temperatures is ~0.6-0.8°C (Fig. 2B; (Willmott &
117 Matsuura, 2001)). Available measurements also indicate low seasonal and interannual variability
118 of lake water temperatures (Harbott et al., 1982; Källqvist et al., 1988; Halfman, 1996).
119 Interannual precipitation variability directly over the lake is below 15 cm/year (Fig. 2B) and
120 exerts a negligible influence on the water mass and stable isotopic budget of Lake Turkana
121 (Ricketts & Johnson, 1996). The Ethiopian highlands and the Omo-Gibe drainage regions
122 encounter much stronger variability in rainfall (Fig. 2D), where rainwater isotope measurements
123 also exhibit large (4-5 ‰, VSMOW) interannual variance (Bedaso et al., 2020).

124 Being the dominant influx to Lake Turkana, Omo River discharge modulates
125 hydrological and geochemical variability in Lake Turkana (Ng'ang'a et al., 1998; Avery &
126 Tebbs, 2018; Ricketts & Johnson, 1996). The rate of Omo River inflow and its geochemical
127 composition influences the mean composition of Lake Turkana, as well as that of carbonates
128 forming from lake waters (Ricketts & Anderson, 1998). Here, the $\delta^{18}O$ of authigenic and
129 biogenic calcite – if precipitated in isotopic equilibrium – reflects the $\delta^{18}O_w$ and the temperature
130 of the water mass at the time of formation (Halfman & Johnson, 1988; Johnson et al., 1991;
131 Ricketts & Anderson, 1998). As temperature variability in the region is relatively minor, $\delta^{18}O_w$
132 has been shown to be the main control on the $\delta^{18}O$ of calcite (Ricketts & Johnson, 1996; Ricketts
133 & Anderson, 1998). $\delta^{18}O_w$ in Lake Turkana is driven by the interplay between 1) the volume of
134 net riverine flows into Lake Turkana (dominated by the Omo River), 2) the $\delta^{18}O$ composition of
135 net inflows, and 3) the rate of evaporation over the lake (Johnson et al., 1991; Ricketts &
136 Johnson, 1996; Ng'ang'a et al., 1998). Precipitation above the lake as well as its $\delta^{18}O$
137 composition negligibly affect the mean composition of Lake Turkana (Ricketts & Johnson,
138 1996). Omo River waters also bring in nutrients in the form of dissolved inorganic carbon (DIC),
139 phosphate, and nitrate into Lake Turkana, and mediate carbon cycling in the lake (Johnson et al.,
140 1991). Accordingly, the $\delta^{13}C$ of DIC in Omo River waters exerts an influence on the $\delta^{13}C$ of

141 calcite precipitated in Lake Turkana (Johnson et al., 1991). Available measurements of
142 productivity in the lake generally delineate a latitudinal trend of decreasing primary production
143 moving away from the northern plume (Government of Kenya and the Ministry of Overseas
144 Development, 1982), additionally establishing the impact of Omo River inflow on Lake Turkana
145 biogeochemistry.

146   Omo-Turkana sediments have been the focus of extensive geochemical study to
147 investigate East African climate change across the Neogene. Geochemical records have been
148 developed from stable isotopes in authigenic carbonates (Halfman & Johnson, 1988; Ricketts &
149 Anderson, 1998; Johnson et al., 1991), biogenic carbonates including ostracodes (Halfman et al.,
150 1989; Beck et al., 2019a; Beck et al., 2021; Ng'ang'a et al., 1998) mollusks (Abell, 1982;
151 Forman et al., 2014; van der Lubbe et al., 2017; Vonhof et al., 2013) and stromatolites (Abell et
152 al., 1982), pedogenic carbonates (Cerling et al., 1988; Levin, 2015; Beck et al., 2019b; Wynn,
153 2004; Quinn & Lepre, 2020), fossil teeth (Cerling et al., 2015; Cerling et al., 2011a), and using
154 organic biomarkers (Uno et al., 2016; Lupien et al., 2018; Lupien et al., 2020; Morrissey &
155 Scholz, 2014; Morrissey et al., 2018). Compared to the extensive studies characterizing modern
156 stable isotope variability in authigenic (Ricketts & Anderson, 1998; Johnson et al., 1991;
157 Halfman & Johnson, 1988; Halfman et al., 1994; Halfman et al., 1989), molluscan (Vonhof et
158 al., 2013; Abell, 1982; van der Lubbe et al., 2017; Manobianco, 2021), and pedogenic carbonates
159 (Cerling et al., 1988; Cerling et al., 2011b; Quinn & Lepre, 2020), to our knowledge, only three
160 studies have investigated multi-specimen analyses of $\delta^{18}O$ and $\delta^{13}C$ for modern ostracodes from
161 Lake Turkana (Ng'ang'a et al., 1998; Halfman et al., 1989), with only 35 previously published
162 values on modern *S. clavularis*. In this work, we provide 329 new IOVA-$\delta^{13}C$ and -$\delta^{18}O$
163 measurements on individual *S. clavularis* specimens in modern sediments collected from Lake
164 Turkana in 1979 and examine seasonal and climatic controls on their intra- and inter-site
165 variance.

166

167 **3. Materials and Methods**

168 **3.1. Sediment Samples and Stable Isotope Analysis**

169   We use surface sediment samples to investigate modern ostracode geochemistry in Lake
170 Turkana. Seventeen sediment samples were used in this study, which were collected across Lake
171 Turkana in July-November 1979, using a modified Ekman dredge with a surface collection area
172 of 225 cm^2 (samples taken from uppermost, biologically active zone-oxidized sediments). At
173 certain sites, surface and bottom water temperatures were recorded; details about sampling
174 methodologies have been reported previously (Cohen, 1984; Cohen, 1986). We note that these
175 samples contained live organisms at the time of collection and that epifauna were isolated from
176 infauna in undisturbed dredge samples (Cohen, 1986), thereby attesting to the modern age of
177 these sediments. Individual calcitic valves of ostracode species *Sclerocypris cf. clavularis*
178 (Cohen, 1986) were identified and picked from the >125 µm size fraction at each site (see Table
179 1 for details). Due to the rapid calcification of ostracode calcite (Turpen & Angell, 1971; Chivas
180 et al., 1986; Roca & Wansard, 1997) and the lack of data implicating a seasonal preference for
181 this species (Cohen, 1986), we assume that most of these valves calcified in the year prior to
182 collection. Although we cannot rule out that these valves did not calcify over several years
183 preceding 1979, sedimentation rates and the intactness of sample fauna suggest that they were
184 not older than a year to a few years at the time of collection (Cohen, 1986).

185   We measured the mass and length (L1) and height (L2) of each valve using a Sartorius
186   Cubis II Ultra-Micro Balance (precision = 0.5 µg) and a MeijiTechno HDZ7000TS Digital Zoom
187   Microscope System (precision = 10 µm) respectively, housed at the Paleo[2] Laboratory at the
188   University of Arizona. Owing to their relatively large masses (average mass of all valves was
189   ~225 µg), valves were then gently cracked using a pin and fragments amounting to 20-80 µg
190   were collected for stable isotopic analysis. IOVA-δ^{13}C and -δ^{18}O (n=329) - with values reported
191   in permil (‰) relative to Vienna Pee Dee Belemnite (VPDB) – were measured using a Kiel IV
192   Carbonate Device coupled to a MAT 253+ isotope ratio mass spectrometer housed at the Paleo[2]
193   Laboratory at the University of Arizona. IAEA-603 standards (n=60) were used to monitor
194   precision over the period of analyses and the reported statistics (δ^{13}C = 2.46 ± 0.03 ‰.; δ^{18}O = -
195   2.37 ± 0.05 ‰) are consistent with the long-term precision of this setup (0.03 ‰ and 0.05 ‰ 1σ
196   for δ^{13}C and δ^{18}O respectively). Intra-valve isotope heterogeneity was confirmed to be negligible
197   as replicate analyses of fragments from an individual valve (n=23) were found to be identical to
198   each other within analytical uncertainty.

3.2. δ^{18}O Equilibrium Considerations

200   To investigate oxygen isotope equilibrium, we used the experimentally determined
201   equation provided by Kim & O'Neil, 1997:

$$1000ln\alpha_{calcite-water} = 18.03 * \left(\frac{10^3}{T}\right) - 32.42 \qquad (1)$$

203   where T is temperature of calcite formation and α is the ^{18}O/^{16}O fractionation factor
204   between calcite and water; note that $1000ln\alpha_{calcite-water} \approx \delta^{18}O_{calcite} - \delta^{18}O_{water}$. In
205   tandem with the collected temperature data, the measured δ^{18}O of ostracode valve calcite (after
206   conversion from VPDB to VSMOW) was used to calculate δ^{18}O$_w$ and compared with
207   measurements of δ^{18}O$_w$ across different years of collection (Cerling et al., 1988; Cerling, 1996;
208   Ricketts & Johnson, 1996).

209   As comprehensive measurements of organic carbon production, carbonate system
210   parameters including alkalinity, DIC, and DIC-δ^{13}C, and nutrient loading data in the Omo River
211   or across Lake Turkana are not available, we refrain from assessing carbon isotope equilibrium
212   constraints using our IOVA-δ^{13}C measurements.

3.3. Influence of Omo River Inflow and Related Statistical Analysis

214   We examined the relative influence of Omo River inflow on our geochemical
215   measurements by calculating a north-to-south distance for each of our sites from a fixed arbitrary
216   marker in the Omo River delta region (Fig. 1B), slightly north of Lake Turkana. Because the
217   sharp bend in the lake precludes making a simple linear measurement from the marker point to
218   the four sites in the southern part of the lake (Sites 79-189F, 79-193F, 79-204F, 79-194F), we
219   added the distance of the initial marker to a fixed point in the central part of the lake (east of Site
220   79-183F) to their relative distances from that point. By assigning a distance (km) from Omo
221   River inflow to each site, we were able to investigate proximity to the Omo River as a control on
222   our measurements. We then applied weighted linear regression using maximum likelihood
223   estimation to calculate the Pearson correlation coefficient and line of best fit (York et al., 2004;
224   Thirumalai et al., 2011). Whereas analytical precision (1σ) was used as error-based weights for
225   the regression across all isotope data (Fig. 3), we used the intra-site standard deviation (1σ_{intra})
226   between individual valves as weights for the inter-site regressions (Figs. 4-5; including for
227   regressions with mass, L1, and L2 – see Table 2). Finally, we compared the calculated δ^{18}O$_w$ at

228 each site (assumed as a baseline for 1979) with direct measurements of $\delta^{18}O_w$ collected in
229 January 1994 (Ricketts & Johnson, 1996) (see Fig. 5). Errors for the inversion of $\delta^{18}O_w$ were
230 propagated using a Monte Carlo procedure (n=1000 for each site), where mean values were
231 allowed to normally vary about the root mean square error calculated using both analytical
232 uncertainty and $1\sigma_{intra}$ at each site (Table 1).

233 **4. Results**

234 **4.1. Negligible Influence of Valve Morphometrics on Stable Isotopes**

235 Pooled statistics (mean and standard deviation) of stable isotopes, mass, valve length
236 (L1), and height (L2) with an average number of ~19 valves analyzed per site, are presented in
237 Table 1. We calculated inter-site correlation coefficients for each of these parameters using the
238 pooled data at each site (Table 2). The average mass, length, and height across all ostracode
239 valves was 225 (±50) µg, 2.09 (±0.11) mm, and 1.09 (± 0.07) mm. We found no significant
240 correlations between stable isotope composition (either $\delta^{13}C$ or $\delta^{18}O$) and valve mass, height, or
241 length across all samples (p > 1 & r^2 < 0.02 across each combination; not shown), or when
242 comparing mean values across each site (Table 2). Owing to significant correlations only
243 amongst other morphometric variables and lack of covariance with stable isotopes, latitude,
244 longitude, depth, and distance (Table 2), we conclude that the *S. clavularis* morphometrics (valve
245 mass, length, and height) do not have a discernable environmental sensitivity nor do they impact
246 the stable isotopic composition of their valve material.

247 **4.2. Inter-site Covariance of Modern *S. clavularis* $\delta^{13}C$ and $\delta^{18}O$ at Lake Turkana**

248 Stable carbon and oxygen isotopes in modern *S. clavularis* at Lake Turkana exhibit a
249 range of ~6 ‰ ($\delta^{13}C_{max}$ = 0.87 ‰; $\delta^{13}C_{min}$ = -5.14 ‰) and ~3.8 ‰ ($\delta^{18}O_{max}$ = 5.37 ‰; $\delta^{18}O_{min}$ =
250 1.59 ‰) relative to VPDB, respectively, across all measured samples (Fig. 3). As is expected for
251 closed-basin lakes (Talbot, 1990), we observe a significant positive correlation between $\delta^{13}C$ and
252 $\delta^{18}O$ (p<0.001; r = 0.54) of ostracode calcite, with the line of best-fit being:

253 $$\delta^{13}C = -10.38 \, (\pm 0.10) + 2.54 \, (\pm 0.03) * \delta^{18}O \qquad (2)$$

254 The range of these values encompasses all previous (albeit multi-specimen and not
255 IOVA) measurements of modern *S. clavularis* $\delta^{18}O$ and $\delta^{13}C$ from Lake Turkana sediments
256 (Ng'ang'a et al., 1998; Halfman et al., 1989). Ng'ang'a and colleagues (1998) found that the
257 average of modern *Hemicypris intermedia* $\delta^{13}C$ and $\delta^{18}O$ (squares in Fig. 3A) was consistently
258 higher than that of *S. clavularis* (circles in Fig. 3A) in Lake Turkana – further confirmed by Beck
259 et al. (2021). Compared to our newly generated *S. clavularis* data (Fig. 3A), collectively, the
260 previously published measurements of *H. intermedia* indeed cluster towards the most positive
261 $\delta^{13}C$ *S. clavularis* values, although $\delta^{18}O$ values ranged within our *S. clavularis* measurements
262 (Fig. 3A). Similarly, $\delta^{18}O$ of modern specimens of *Potamocypris worthingtoni* were within range
263 of all available *S. clavularis* $\delta^{18}O$, although $\delta^{13}C$ was systematically higher (Fig. 3A triangles).
264 This could be related to the fact that most of the multi-specimen measurements presented in
265 Beck et al. (2021) were sampled from shallow regions of the lake (~3-5 m) or from beaches.
266 However, *P. worthingtoni* is also known to be a shallow water dweller, which could additionally
267 explain the higher $\delta^{13}C$ values of this species (Cohen, 1986). The average *S. clavularis* $\delta^{13}C$ and
268 $\delta^{18}O$ values in our study (n=329) were -1.71 and 3.38 ‰. We note that the average $\delta^{13}C$ (-2.08

269   ‰; n = 35) and $\delta^{18}O$ (3.13 ‰; n = 35) in previous studies (Ng'ang'a et al., 1998; Halfman et al.,

270   1989) are offset relative to our samples by ~0.2 ‰ and ~0.3 ‰ respectively, which may be

271   related to more limited spatial sampling. Overall, previous multi-specimen *S. clavularis* $\delta^{13}C$ and

272    $\delta^{18}O$ are consistent with the range of our IOVA measurements.

273   When we pool our *S. clavularis* measurements by location (n=17; Fig. 3B), the range of

274   mean IOVA values spans 2.27 ‰ (VPDB) in $\delta^{13}C$ and 2.01 ‰ (VPDB) in $\delta^{18}O$ across the sites,

275   with lower values in the northern part of the lake. The positive correlation between site-based

276   mean IOVA-$\delta^{13}C$ and -$\delta^{18}O$ becomes stronger (p<0.001; r = 0.75) relative to the regression

277   containing all measured samples (Fig. 3A-B). The inter-site pooled means exhibit a line of best-

278   fit having an intercept closer to zero and a lower $\delta^{13}C$-$\delta^{18}O$ slope than that constructed with all

279   measurements, albeit with higher uncertainty due to the incorporation of within-site variability

280   ($1\sigma_{intra}$) as errors (Fig. 3b):

281
$$\delta^{13}C = -5.21\,(\pm 1.73) + 1.02\,(\pm 0.51) * \delta^{18}O \tag{3}$$

282   Mean IOVA-$\delta^{13}C$ and -$\delta^{18}O$ values across the sites show significant correlations (Table 2)

283   with depth (both $\delta^{13}C$ and $\delta^{18}O$), latitude (both $\delta^{13}C$ and $\delta^{18}O$), and longitude (only $\delta^{18}O$).

284   However, we find that the omission of the four southernmost sites bring about reductions in

285   covariance with depth (r^2 reduces from 0.78 to 0.46 for $\delta^{18}O$, and from 0.32 to 0.31 for $\delta^{13}C$) and

286   longitude (r^2 reduces from 0.46 to 0 for $\delta^{18}O$ and remains unchanged at 0.06 for $\delta^{13}C$). It is worth

287   noting that the southern basin veers towards the east and is notably deeper than the north such

288   that correlations with longitude are driven by the shape of the lake. Nevertheless, correlations

289   with latitude remain high with (r^2 = 0.55 for $\delta^{18}O$; r^2 = 0.31 for $\delta^{13}C$) or without omission (r^2 =

290   0.78 for $\delta^{18}O$; r^2 = 0.32 for $\delta^{13}C$) of the four southern sites.

291   **4.3. Similar Intra-Site Stable Isotopic Variance Across Lake Turkana Sites**

292   At all sites we find larger IOVA-$\delta^{13}C$ variance than that of IOVA-$\delta^{18}O$ (Table 1). $\delta^{18}O$

293   variability at each site (*i.e.*, $1\sigma_{intra}$) ranges from 0.28 ‰ (Site 79-166F) to 0.57 ‰ (Site 79-193F),

294   whereas inter-site $\delta^{13}C$ variability ranges from 0.68 ‰ (Site 79-166F) to 1.32 ‰ (Site 79-183F).

295   Additionally, we note that these two parameters themselves are not significantly correlated

296   across sites (Table 2), nor are they correlated with water depth, longitude, latitude, or distance

297   from Omo River inflow. Average IOVA-$\delta^{13}C$ and -$\delta^{18}O$ $1\sigma_{intra}$ across all sites combined is 1.00

298   (± 0.21) ‰ and 0.42 (± 0.10) ‰, indicating that the mean $1\sigma_{intra}$ is larger than site-to-site stable

299   isotope variance. This observation is consistent with the inference that ostracode valve

300   calcification across the entire lake encounters similar carbon and oxygen isotope variability,

301   despite different inter-site mean values.

302   **4.4. Near-Equilibrium Oxygen Isotope Calcification of *S. clavularis***

303   We compiled available measurements of modern $\delta^{18}O_w$ at Lake Turkana (Cerling, 1996;

304   Cerling et al., 1988; Ricketts & Anderson, 1998) alongside our ostracode $\delta^{18}O$ and *in situ* bottom

305   water temperature measurements (Cohen, 1981; Cohen, 1984) to determine whether ostracode

306   calcification took place under isotopic equilibrium. In total, we compiled thirty seven published

307    $\delta^{18}O_w$ values whose average $\delta^{18}O$ is 5.72 $\pm$ 0.71 (1σ) ‰ (reported relative to VSMOW) collected

308   from the lake across different years, comprised of three samples collected in September 1975,

309   March 1977, and August 1980 (Cerling et al., 1988) (locations unknown; average ä¹⁸O$_w$ = 5.83
310   ‰), 17 samples collected between September 1980 and September 1982 (average $\delta^{18}O_w$ = 6.1
311   ‰) at the Koobi Fora spit (Cerling, 1996) located south of our sampling site BS-91 on the
312   eastern flank of the lake (Fig. 2), and 17 samples collected across various sites along the lake
313   (Ricketts & Johnson, 1996) in January 1994 (average $\delta^{18}O_w$ = 5.48 ‰). $\delta^{18}O_w$ data from Ricketts
314   and Johnson (1996) clearly delineate a north-to-south trend towards ¹⁸O enrichment away from
315   the Omo River inflow (green points in Fig. 5A) and confirm the importance of changing $\delta^{18}O_w$ as
316   a contributor of calcite $\delta^{18}O$ precipitation across the lake. Thus, to minimize biases associated
317   with ephemeral spatiotemporal $\delta^{18}O_w$ sampling across the lake and to maximize available
318   measurements, we focus on a sub-selection of *in situ* temperature, IOVA-$\delta^{18}O$, and $\delta^{18}O_w$
319   samples collected north of the Koobi Fora spit to assess isotopic equilibrium.

320   The average $\delta^{18}O_w$ of available samples (n_{sites} = 2; n_{total} = 19) across the northern portion
321   (>3.9°N) of Lake Turkana is 5.86 ± 0.56 (1σ) ‰ (VSMOW) which, coupled with average *S.*
322   *clavularis* $\delta^{18}O$ of 2.98 ± 0.28 (1σ) ‰ (VPDB; n_{sites} = 6; n_{total} = 105) in this domain yields an
323   average calcification temperature of 25.3 ± 2.8 °C (1σ propagated error) using equation (1); this
324   estimate is virtually identical to average *in situ* bottom water measurements (n_{sites} = 4; n_{total} = 4)
325   of 25.3 ± 1.5 (1σ) °C (Table 3). We note that even this sub-selection of samples may not be an
326   appropriate "apples to apples" comparison for equilibrium constraints as coevally collected
327   ostracodes, bottom water temperature, and $\delta^{18}O_w$ data do not exist. If we focus solely on IOVA-
328   $\delta^{18}O$ measurements at BS-90 and BS-91 (average $\delta^{18}O$ = 3.11 ± 0.5 ‰; n_{total} = 34), proximal to
329   the Koobi Fora spit, and apply the nearest *in situ* bottom-water temperature (23.5 °C at site 79-
330   168F; 36 km away), we obtain a $\delta^{18}O_w$ estimate of 5.73 ± 0.51 (1σ propagated error) ‰
331   (VSMOW; see Table 3). This reconstructed value is identical within uncertainty to the average
332   $\delta^{18}O_w$ of 5.74 ± 0.57 (1σ) ‰ (VSMOW), measured at that location (n_{total} = 17), although we
333   further caution that the Koobi Fora water samples were collected long after our 1979 sample
334   collection (Cerling, 1996). Assuming that the average bottom-water temperature of calcification
335   for ostracodes across the entire lake to be 25.7°C (the average of our *in situ* bottom water
336   measurements), the average IOVA-$\delta^{18}O$ of all our measurements (3.40 ‰; n = 352) points to a
337   mean Turkana $\delta^{18}O_w$ value of 6.4 ± 0.5 ‰ for 1979 (*i.e.,* over the average duration of
338   calcification of ostracode valves in our sample), which is within the range of $\delta^{18}O_w$ (4.75 - 8.95
339   ‰) measured in subsequent years. Finally, we note that if we pool all available $\delta^{18}O_w$
340   measurements (n=17) along with all ostracode $\delta^{18}O$ measurements (n=329), we obtain a mean
341   bottom-water temperature estimate of 22.5 °C with a propagated uncertainty of ±3.8 °C (Table
342   3). Although within uncertainty, this median estimate is cooler than most available
343   measurements (Harbott et al., 1982; Cohen, 1986; Källqvist et al., 1988) and suggests that
344   inaccuracies may arise due to the lack of *in situ* bottom water $\delta^{18}O_w$ measurements paired with
345   ostracode calcite $\delta^{18}O$.

346   Overall, our data are consistent with the average $\delta^{18}O$ of numerous individual valves
347   being deposited at apparent (or near) equilibrium conditions. Considering sampling uncertainty
348   in the other parameters, we cannot rule out small deviations from equilibrium on the order of
349   ~0.2-0.3 ‰ (VPDB). That said, our analysis rules out that *S. clavularis* $\delta^{18}O$ deviates from
350   equilibrium by 0.5-1.5 ‰, as hypothesized previously (Ng'ang'a et al., 1998) using a much
351   smaller number of samples (Fig. 3). Although future coeval sampling may provide more precise

352 insights, we conclude that IOVA-δ^{18}O measurements in tandem with available environmental
353 data are consistent with calcification close to oxygen isotope equilibrium.

4.5. Large Intra-Site and Inter-Site IOVA-δ^{13}C Variability

355 IOVA-δ^{13}C across Lake Turkana samples range from 0.87 ‰ to -5.14 ‰ (~6‰),
356 exhibiting large intra-site variability (average intra-site $1\sigma = 1 \pm 0.21$ ‰; Table 1), with an
357 average value of -1.75 ‰. The average intra-site standard deviation of IOVA-δ^{13}C values is more
358 than double of its IOVA-δ^{18}O counterpart, and points towards more complex controls. Amongst
359 other factors, ostracode δ^{13}C is influenced by DIC-δ^{13}C values in waters where they calcify (Xia
360 et al., 1997; Pérez et al., 2013), which can be driven by ^{13}C enrichment due to primary
361 productivity (Källqvist et al., 1988) or due to varying riverine δ^{13}C inputs. However, dietary
362 preferences can also alter ostracode δ^{13}C (Limén & Olafsson, 2002) – a process which may be
363 particularly relevant to *S. clavularis*, which feeds on organic detritus (Cohen, 1986). Whereas
364 higher surface production and organic matter consumption lead to lower benthic δ^{13}C (Källqvist
365 et al., 1988; Pérez et al., 2013), out-of-phase seasonal stratification and Omo River
366 inflow(Källqvist et al., 1988), could explain the large variance in IOVA-δ^{13}C. Nevertheless,
367 mean IOVA-δ^{13}C across sites yield a significant slope of 0.1 ‰ (VPDB) per 10 km that mirrors
368 the δ^{18}O slope (Fig. 4), despite higher uncertainty owing to high $1\sigma_{intra}$ for δ^{13}C between valves.
369 This observation points to the Omo River influx as the main driver of the spatial patterns of both
370 IOVA-δ^{18}O and δ^{13}C across our sites.

5. Discussion

372 Our IOVA datasets reveal a strong imprint of Omo River inflow on Lake Turkana
373 geochemistry. The observed latitudinal trends across mean IOVA values arises due to the north-
374 south geometry of the lake basin and the southward dissipation of the Omo River plume into the
375 lake (Fig. 4). Accordingly, we find that using distance from Omo River inflow as a predictor
376 yields the strongest correlations with mean IOVA-δ^{13}C ($r^2 = 0.33$) and δ^{18}O ($r^2 = 0.81$) values
377 (Table 2). Considering near-equilibrium calcification for δ^{18}O (see Section 4.4) and assuming the
378 same for δ^{13}C, inter-site IOVA means exhibit more enriched ^{18}O and ^{13}C of ostracode calcite
379 towards the southern part of the lake and support that low-δ^{18}O/δ^{13}C Omo River waters (Cerling
380 et al., 1988) modulate mean stable isotopic variability across Lake Turkana.

381 Superimposed on the southward waning of the low-δ^{18}O Omo River plume, ^{18}O
382 enrichment in ostracode calcite is linked to evaporation over the lake (green dots in Fig. 5A),
383 which additionally serves to heighten $\delta^{18}O_w$ (Cerling et al., 1988; Cerling, 1996; Johnson et al.,
384 1991; Ricketts & Johnson, 1996). Assuming a mean temperature of calcification (25.7°C) based
385 on all available bottom water temperature measurements from 1979 (and applying a 1°C north-
386 south difference to the four southern-most sites), we calculated $\delta^{18}O_w$ from our inter-site IOVA-
387 δ^{18}O dataset (orange points in Fig. 5A). This yields a reconstructed $\delta^{18}O_w$ range of ~1.8 ‰
388 (VSMOW), which is similar to the range measured by Ricketts and Johnson (1996) across the
389 lake in January 1994 (~1.31 ‰); we note that their sampling range did not extend as far south as
390 ours, and if we limit our samples to their same range (based on distance from Omo River
391 inflow), our reconstructed $\delta^{18}O_w$ range becomes ~1.2 ‰ (*i.e.,* omitting the northernmost and
392 southernmost values; see Fig. 5). Despite similar ranges and slopes however, the reconstructed
393 inter-site $\delta^{18}O_w$ for samples collected in 1979 are offset, on average, by 0.9 ‰ relative to

394 measurements in January 1994 (Fig. 5A). As the Omo River is ultimately sourced from
395 precipitation in the Ethiopian highlands, for illustrative purposes, we investigated mean annual
396 precipitation anomalies between 1979 and 1993 (*i.e.*, the year preceding January 1994; Fig. 5B)
397 as a cause for the $\delta^{18}O_w$ offset using monthly GPCC station-based rainfall data (Beck et al.,
398 2005). Interestingly, we find that the northern portion of the Omo catchment received far more
399 precipitation (>20 cm) in 1993 relative to 1979 whereas surrounding catchments of other rivers
400 that do not drain into Turkana were anomalously dry (Fig. 5B). Thus, increased rainfall in the
401 Ethiopian highlands during 1993 relative to 1979 could explain the offset in $\delta^{18}O_w$ between the
402 years – either via increased volume of Omo River discharge or via more negative $\delta^{18}O$ of Omo
403 River waters fed by more negative $\delta^{18}O$ of precipitation (Ricketts & Anderson, 1998). We
404 caution that this exercise unrealistically simplifies several hydrometeorological complexities of
405 $\delta^{18}O$ fractionation including processes related to seasonality, clouds, spatial variability in riverine
406 discharge, catchment storage etc. (Bedaso et al., 2020; Dasgupta et al., 2021; Maupin et al.,
407 2021). Nevertheless, it provides confidence in using IOVA-$\delta^{18}O$ to reconstruct lake water $\delta^{18}O_w$
408 and its links with rainfall from where the Omo River is sourced. Future research may refine the
409 quantitative relationship between Ethiopian rainfall $\delta^{18}O$, Omo River discharge, and IOVA-
410 reconstructed lake water $\delta^{18}O_w$. Overall, our data are consistent with higher precipitation in the
411 Omo catchment leading to lowered Lake Turkana $\delta^{18}O_w$, as proposed before (Halfman &
412 Johnson, 1988; Johnson et al., 1991; Ricketts & Johnson, 1996).

413   Whereas few carbonate system measurements exist to sufficiently investigate controls on
414 ostracode $\delta^{13}C$ across Lake Turkana, co-variance between inter-site mean IOVA-$\delta^{13}C$ with
415 distance from inflow (Fig. 4B) suggest an Omo River control. We suggest that such a trend
416 towards positive $\delta^{13}C$ values towards the southern part of the lake could arise due to two possible
417 effects: 1) dilution of low-$\delta^{13}C$ values of the Omo River plume (Johnson et al., 1991), and 2)
418 dilution of nutrients associated with the riverine plume leading to lower primary production
419 (Government of Kenya and the Ministry of Overseas Development, 1982; Källqvist et al., 1988)
420 and hence, higher DIC-$\delta^{13}C$ in bottom waters towards the southern part of the lake owing to
421 lower amounts of microbially mediated breakdown of organic matter. Although no direct
422 measurements of DIC-$\delta^{13}C$ exist for the Omo River, its $\delta^{13}C$ likely falls between -5 to -15 ‰ in
423 accordance with other East African river waters (Cerling et al., 1988; Johnson et al., 1991) – far
424 more negative than measured lake water DIC-$\delta^{13}C$, which range between 0 and -1 ‰ at the
425 Koobi Fora spit (Cerling, 1996). Production in Turkana is N-limited (Källqvist et al., 1988), and
426 Omo River inflow brings large amounts of nitrates into the lake that cause blooms towards the
427 north (Källqvist et al., 1988; Avery & Tebbs, 2018). Here, it may be likely that organic matter
428 $\delta^{13}C$ is highly negative due to large photosynthetic fractionation (Hodell & Schelske, 1998), and
429 microbial breakdown of organic matter would result in low-$\delta^{13}C$ bottom water DIC, which
430 imprints itself onto benthic ostracode calcite (Pérez et al., 2013). Moreover, considering that *S.*
431 *clavularis* is a detritivore feeding on deposited particulate organic matter (Cohen, 1986), the
432 carbon isotopic composition of its diet could imprint its $\delta^{13}C$ on the ostracode valve during
433 calcification (*i.e.*, a "vital effect"). Both dilution effects are consistent with our observation of
434 higher mean IOVA-$\delta^{13}C$ towards the southern part of the lake. Complex interactions between
435 these effects could confound straightforward interpretations of IOVA-$\delta^{13}C$ and may in part
436 explain the high variance we observe. As one example, wind-driven mixing during seasons
437 outside that of riverine pulses could regenerate nutrients in surface waters from the deep and
438 promote primary production. Thus, we recommend caution in downcore interpretations of
439 IOVA-$\delta^{13}C$ linked solely to primary production. Taken together, the mean IOVA-$\delta^{13}C$ and $1\sigma_{intra}$

440   of our measurements (2.11 ± 0.1 ‰, VPDB) provide a modern reference for future IOVA-δ^{13}C
441   applications.

442   Overall, our results suggest that pooled averages of IOVA measurements can accurately
443   reflect mean limnological conditions in Lake Turkana, and hence IOVA may be an effective tool
444   to infer paleotemperature and paleohydrology in the region. However, site-based IOVA values
445   also capture the large spatial variability across the lake, on the order of several permille in both
446   IOVA-δ^{18}O and -δ^{13}C (Fig. 4). As this basin is thought to have encountered large lake-level
447   changes over the Holocene and Pleistocene – changes that may have decoupled the northern and
448   southern parts of the basin (Bloszies et al., 2015) – we suggest that downcore investigations of
449   IOVA at Lake Turkana and related inferences about paleohydrology be conducted with this
450   spatial dimension in mind, in addition to analyzing large numbers of valves.

451   Can IOVA-δ^{18}O be used to reconstruct interannual hydroclimate variability or its
452   seasonality? The average $1\sigma_{intra}$ for ostracode δ^{18}O measurements across all sites is 0.42 ± 0.10
453   ($1\sigma_{\sigma\text{-intra}}$) ‰ (VPDB; Table 1). The average year-to-year (1σ) temperature variability across the
454   lake is ~0.45 °C (Fig. 2B), and the standard deviation of climatological seasonal cycle of
455   temperature is ~0.7 °C (not shown). If we assume that these parameters are accurate for bottom
456   water temperatures (which is likely an overestimate), this could explain up to ~0.18 ‰ (VPDB)
457   of the average $1\sigma_{intra}$ values, using a slope of 0.22 ‰/°C and the root mean square estimate for
458   combining both forms of variability (Kim & O'Neil, 1997). Thus, the remaining ~0.24 ‰,
459   amounting to ~60% of the average IOVA-δ^{18}O $1\sigma_{intra}$, must arise from processes related to $\delta^{18}O_w$
460   and hydroclimate changes. Our attribution of temperature versus hydroclimatic variability is
461   probably an underestimate as our samples are not likely to record multiple years of data to
462   capture the full range of interannual variability (see Materials and Methods). We suggest that
463   IOVA-δ^{18}O applied to downcore sediments may be compared to our modern baseline value of
464   variability (0.42 ± 0.10 ‰) to examine whether seasonality or interannual variability of
465   temperature and hydroclimate at Lake Turkana was altered during past periods.

466   **6. Conclusions**

467   We propose that with enough analyses to overcome inter-specimen isotopic variance
468   (n>~20), IOVA of *S. clavularis* in Lake Turkana sediments can be a highly skillful indicator of
469   mean limnological and hydrological conditions and variability in the region. IOVA-δ^{18}O
470   measurements (n=392) from various sites across the lake match well with available *in situ*
471   observations of bottom water temperature ($\delta^{18}O_w$) and are consistent with being deposited under
472   near-equilibrium conditions. Average IOVA-δ^{13}C and -δ^{18}O are highly correlated with each other
473   (Fig. 3), and with proximity to Omo River inflow (Fig. 4), revealing a dominant river-plume
474   influence on Lake Turkana biogeochemistry. We conclude that IOVA performed at Lake
475   Turkana can accurately reflect the hydrological history of Omo River source-waters in the
476   Ethiopian highlands.

477   **Acknowledgements**

481 (TRIF). All data from this study are available in the supplementary section and are in the process
482 of being uploaded to an appropriate online data repository.

483
484 **References**
485

486 Abell, P. I. (1982). Palaeoclimates at Lake Turkana, Kenya, from oxygen isotope ratios of
487   gastropod shells. *Nature*, *297*(5864), 321-323. https://www.nature.com/articles/297321a0
488 Abell, P. I., Awramik, S. M., Osborne, R. H., & Tomellini, S. (1982). Plio-Pleistocene lacustrine
489   stromatolites from Lake Turkana, Kenya: morphology, stratigraphy and stable isotopes.
490   *Sedimentary Geology*, *32*(1-2), 1-26.
491   http://citeseerx.ist.psu.edu/viewdoc/download?doi=10.1.1.710.2024&rep=rep1&type=pdf
492 Avery, S. T., & Tebbs, E. J. (2018). Lake Turkana, major Omo River developments, associated
493   hydrological cycle change and consequent lake physical and ecological change. *Journal of*
494   *Great Lakes Research*, *44*(6), 1164-1182. https://doi.org/10.1016/j.jglr.2018.08.014
495 Beck, C., Grieser, J., & Rudolf, B. (2005). A new monthly precipitation climatology for the
496   global land areas for the period 1951 to 2000. *Geophysical Research Abstracts*, *7*(07154).
497   http://www.juergen-
498   grieser.de/publications/publications_pdf/Beck_Grieser_Rudolf_EGU_05.pdf
499 Beck, C. C., Feibel, C. S., Wright, J. D., & Mortlock, R. A. (2019a). Onset of the African humid
500   period by 13.9 kyr BP at Kabua Gorge, Turkana Basin, Kenya. *The Holocene*, *29*(6), 1011-
501   1019. https://journals.sagepub.com/doi/pdf/10.1177/0959683619831415
502 Beck, C. C., Allen, M. M., Feibel, C. S., Beverly, E. J., Stone, J. R., Wegter, B., & Wilson, C. L.
503   (2019b). Living in a swampy paradise: Paleoenvironmental reconstruction of an African
504   Humid Period lacustrine margin, West Turkana, Kenya. *Journal of African Earth Sciences*,
505   *154*, 20-34. https://doi.org/10.1016/j.jafrearsci.2019.03.007
506 Beck, C. C., Feibel, C. S., Mortlock, R. A., Quinn, R. L., & Wright, J. D. (2021). Little Ice Age
507   to modern lake-level fluctuations from Ferguson's Gulf, Lake Turkana, Kenya, based on
508   sedimentology and ostracod assemblages. *Quaternary Research*, 1-14.
509   https://doi.org/10.1017/qua.2020.105
510 Bedaso, Z. K., DeLuca, N. M., Levin, N. E., Zaitchik, B. F., Waugh, D. W., Wu, S.-Y., Harman,
511   C. J., & Shanko, D. (2020). Spatial and temporal variation in the isotopic composition of
512   Ethiopian precipitation. *Journal of Hydrology*, *585*, 124364.
513   https://doi.org/10.1016/j.jhydrol.2019.124364
514 Bloszies, C., Forman, S. L., & Wright, D. K. (2015). Water level history for Lake Turkana,
515   Kenya in the past 15,000years and a variable transition from the African Humid Period to
516   Holocene aridity. *Global and Planetary Change*, *132*, 64-76.
517   https://doi.org/10.1016/j.gloplacha.2015.06.006
518 Cerling, T. E., Andanje, S. A., Blumenthal, S. A., Brown, F. H., Chritz, K. L., Harris, J. M., Hart,
519   J. A., Kirera, F. M., Kaleme, P., Leakey, L. N., Leakey, M. G., Levin, N. E., Manthi, F. K.,
520   Passey, B. H., & Uno, K. T. (2015). Dietary changes of large herbivores in the Turkana
521   Basin, Kenya from 4 to 1 Ma. *Proc Natl Acad Sci U S A*, *112*(37), 11467-11472.
522   https://doi.org/10.1073/pnas.1513075112
523 Cerling, T. E., Levin, N. E., & Passey, B. H. (2011a). Stable isotope ecology in the Omo-
524   Turkana Basin. *Evol Anthropol*, *20*(6), 228-237. https://doi.org/10.1002/evan.20326
525 Cerling, T. E., Wynn, J. G., Andanje, S. A., Bird, M. I., Korir, D. K., Levin, N. E., Mace, W.,
526   Macharia, A. N., Quade, J., & Remien, C. H. (2011b). Woody cover and hominin

527   environments in the past 6 million years. *Nature*, *476*(7358), 51-56.
528   https://doi.org/10.1038/nature10306
529   Cerling, T. E. (1996). Pore water chemistry of an alkaline rift valley lake: Lake Turkana, Kenya.
530   In T. C. Johnson, Odada, EO (Ed.), *The Limnology, Climatology, and Paleoclimatology of*
531   *the East African Lakes* (pp. 225-240). Univ. of Utah, Salt Lake City (USA).
532   Cerling, T. E., Bowman, J. R., & O'Neil, J. R. (1988). An isotopic study of a fluvial-lacustrine
533   sequence: the Plio-Pleistocene Koobi Fora sequence, East Africa. *Palaeogeography,*
534   *palaeoclimatology, palaeoecology*, *63*(4), 335-356.
535   https://www.sciencedirect.com/science/article/pii/0031018288901046
536   Chivas, A. R., Deckker, P. D., & Shelley, J. M. G. (1986). Magnesium and strontium in non-
537   marine ostracod shells as indicators of palaeosalinity and palaeotemperature.
538   *Hydrobiologia*, *143*, 135-142. https://link.springer.com/chapter/10.1007/978-94-009-4047-
539   5_20
540   Cohen, A. S. (1981). Paleolimnological research at Lake Turkana, Kenya. *Palaeoecology of*
541   *Africa*, *13*(1981), 61-82.
542   Cohen, A. S. (1984). Effect of zoobenthic standing crop on laminae preservation in tropical lake
543   sediment, Lake Turkana, East Africa. *Journal of Paleontology*, *58, No. 2, Trace Fossils*
544   *and Paleoenvironments: Marine Carbonate, Marginal Marine Terrigenous and*
545   *Continental Terrigenous Settings*(Mar., 1984), 499-510. https://doi.org/10.2307/1304798
546   Cohen, A. S. (1986). Distribution and faunal associations of benthic invertebrates at Lake
547   Turkana, Kenya. *Hydrobiologia*, *141*(3), 179-197.
548   https://link.springer.com/article/10.1007/BF00014214
549   Dasgupta, B., Ajay, A., Kumar, A., Thamban, M., & Sanyal, P. (2021). Isoscape of Surface
550   Runoff in High Mountain Catchments: An Alternate Model for Meteoric Water
551   Characterization and Its Implications. *Journal of Geophysical Research: Atmospheres*,
552   *126*(16). https://doi.org/10.1029/2020jd033950
553   Dettman, D. L., Smith, A. J., Rea, D. K., Moore Jr, T. C., & Lohmann, K. C. (1995). Glacial
554   meltwater in Lake Huron during early postglacial time as inferred from single-valve
555   analysis of oxygen isotopes in ostracodes. *Quaternary Research*, *43*(3), 297-310.
556   http://scholar.google.com/scholar?output=instlink&nossl=1&q=info:t4iweW9qlHEJ:schola
557   r.google.com/&hl=en&as_sdt=0,3&scillfp=3085559159630797961&oi=lle
558   Dettman, D. L., Palacios-Fest, M. R., Nkotagu, H. H., & Cohen, A. S. (2005). Paleolimnological
559   investigations of anthropogenic environmental change in Lake Tanganyika: VII. Carbonate
560   isotope geochemistry as a record of riverine runoff. *Journal of Paleolimnology*, *34*(1), 93-
561   105. https://doi.org/10.1007/s10933-005-2400-x
562   Dixit, Y., Hodell, D. A., Sinha, R., & Petrie, C. A. (2014). Abrupt weakening of the Indian
563   summer monsoon at 8.2 kyr B.P. *Earth and Planetary Science Letters*, *391*, 16-23.
564   https://doi.org/10.1016/j.epsl.2014.01.026
565   Dixit, Y., Hodell, D. A., Sinha, R., & Petrie, C. A. (2015). Oxygen isotope analysis of multiple,
566   single ostracod valves as a proxy for combined variability in seasonal temperature and lake
567   water oxygen isotopes. *Journal of Paleolimnology*, *53*(1), 35-45.
568   https://doi.org/10.1007/s10933-014-9805-3
569   Escobar, J., Curtis, J. H., Brenner, M., Hodell, D. A., & Holmes, J. A. (2010). Isotope
570   measurements of single ostracod valves and gastropod shells for climate reconstruction:
571   evaluation of within-sample variability and determination of optimum sample size. *Journal*
572   *of Paleolimnology*, *43*(4), 921-938. https://doi.org/10.1007/s10933-009-9377-9

573 Forman, S. L., Wright, D. K., & Bloszies, C. (2014). Variations in water level for Lake Turkana
574   in the past 8500 years near Mt. Porr, Kenya and the transition from the African Humid
575   Period to Holocene aridity. *Quaternary Science Reviews*, *97*, 84-101.
576   https://www.sciencedirect.com/science/article/pii/S0277379114001747
577 Government of Kenya and the Ministry of Overseas Development, L. (1982). Studies On Algal
578   Dynamics And Primary Productivity. In A. J. Hopson (Ed.), *Lake Turkana: A Report on the*
579   *Findings of the Lake Turkana Project 1972-1975* (Vol. 1, pp. 109-162). Institute of
580   Aquaculture, University of Stirling.
581   https://archive.org/details/laketurkanarepor1198hops/page/n5/mode/2up
582 Halfman, J. D. (1996). CTD-transmissometer profiles from Lakes Malawi and Turkana. *The*
583   *Limnology, Climatology and Paleoclimatology of the East African Lakes*, 169-182.
584 Halfman, J. D., & Johnson, T. C. (1988). High-resolution record of cyclic climatic change during
585   the past 4 ka from Lake Turkana, Kenya. *Geology*, *16*(6), 496-500.
586   https://pubs.geoscienceworld.org/geology/article-lookup/16/6/496
587 Halfman, J. D., Johnson, T. C., & Finney, B. P. (1994). New AMS dates, stratigraphic
588   correlations and decadal climatic cycles for the past 4 ka at Lake Turkana, Kenya.
589   *Palaeogeography, Palaeoclimatology, Palaeoecology*, *111*(1-2), 83-98.
590   https://www.sciencedirect.com/science/article/pii/0031018294903492
591 Halfman, J. D., Johnson, T. C., Showers, W. J., & Lister, G. S. (1989). Authigenic low-Mg
592   calcite in Lake Turkana, Kenya. *Journal of African Earth Sciences (and the Middle East)*,
593   *8*(2-4), 533-540. https://www.sciencedirect.com/science/article/pii/S0899536289800430
594 Harbott, B. J., Ferguson, A. J. D., & Hopson, A. J. (1982). *The Lake Turkana Fisheries*
595   *Research Project 1972-1975. A Summary Of The Findings*. In.
596 Heaton, T. H. E., Holmes, J. A., & Bridgwater, N. D. (1995). Carbon and oxygen isotope
597   variations among lacustrine ostracods: implications for palaeoclimatic studies. *The*
598   *Holocene*, *5*(4), 428-434.
599   https://journals.sagepub.com/doi/pdf/10.1177/095968369500500405
600 Hodell, D. A., & Schelske, C. L. (1998). Production, sedimentation, and isotopic composition of
601   organic matter in Lake Ontario. *Limnology and Oceanography*, *43*(2), 200-214.
602   https://aslopubs.onlinelibrary.wiley.com/doi/abs/10.4319/lo.1998.43.2.0200
603 Holmes, J. A., Street-Peffott, F. A., Ivanovich, M., & Peffott, R. A. (1995). A late Quaternary
604   palaeolimnological record from Jamaica based on trace-element chemistry of ostracod
605   shells. *Chemical Geology*, *124*(1-2), 143-160.
606   https://www.sciencedirect.com/science/article/pii/000925419500032H
607 Holmes, J. A. (2008). Sample-size implications of the trace-element variability of ostracod
608   shells. *Geochimica et Cosmochimica Acta*, *72*(12), 2934-2945.
609   https://doi.org/10.1016/j.gca.2008.03.020
610 Johnson, T. C., Halfman, J. D., & Showers, W. J. (1991). Paleoclimate of the past 4000 years at
611   Lake Turkana, Kenya, based on the isotopic composition of authigenic calcite.
612   *Palaeogeography, Palaeoclimatology, Palaeoecology*, *85*(3-4), 189-198.
613   https://www.sciencedirect.com/science/article/pii/003101829190158N
614 Källqvist, T., Lien, L., & Liti, D. (1988). Lake Turkana limnologlcal study 1985-1988.
615   *Norwegian Institute for Water Research & Kenya Marine and Fisheries Research Institute*.
616   https://aquadocs.org/bitstream/handle/1834/6965/ktf0339.pdf?sequence=2

617 Kim, S.-T., & O'Neil, J. R. (1997). Equilibrium and nonequilibrium oxygen isotope effects in
618   synthetic carbonates. *Geochimica et Cosmochimica Acta*, *61*(16), 3461-3475.
619   https://doi.org/10.1016/s0016-7037(97)00169-5
620 Last, W. M., Teller, J. T., & Forester, R. M. (1994). Paleohydrology and paleochemistry of Lake
621   Manitoba, Canada: the isotope and ostracode records. *Journal of Paleolimnology*, *12*(3),
622   269-282. https://link.springer.com/article/10.1007/BF00678025
623 Levin, N. E. (2015). Environment and Climate of Early Human Evolution. *Annual Review of
624   Earth and Planetary Sciences*, *43*(1), 405-429. https://doi.org/10.1146/annurev-earth-
625   060614-105310
626 Limén, H., & Ólafsson, E. (2002). Ostracod species-specific utilisation of sediment detritus and
627   newly settled cyanobacteria, *Aphanizomenon* sp., in the Baltic Sea: evidence from stable
628   carbon isotopes. *Marine Biology*, *140*(4), 733-738. https://doi.org/10.1007/s00227-001-
629   0739-8
630 Lupien, R. L., Russell, J. M., Feibel, C., Beck, C., Castañeda, I., Deino, A., & Cohen, A. S.
631   (2018). A leaf wax biomarker record of early Pleistocene hydroclimate from West Turkana,
632   Kenya. *Quaternary Science Reviews*, *186*, 225-235.
633   https://doi.org/10.1016/j.quascirev.2018.03.012
634 Lupien, R. L., Russell, J. M., Grove, M., Beck, C. C., Feibel, C. S., & Cohen, A. S. (2020).
635   Abrupt climate change and its influences on hominin evolution during the early Pleistocene
636   in the Turkana Basin, Kenya. *Quaternary Science Reviews*, *245*, 106531.
637   https://doi.org/10.1016/j.quascirev.2020.106531
638 Manobianco, J. A. (2021). Interpretation of Seasonality from Geochemistry and
639   Sclerochronology of Holocene and Pleistocene Freshwater Bivalves from the Omo-
640   Turkana Basin, Ethiopia and Kenya.
641 Maupin, C. R., Roark, E. B., Thirumalai, K., Shen, C.-C., Schumacher, C., Van Kampen-Lewis,
642   S., Housson, A. L., McChesney, C. L., Baykara, O., Yu, T.-L., White, K., & Partin, J. W.
643   (2021). Abrupt Southern Great Plains thunderstorm shifts linked to glacial climate
644   variability. *Nature Geoscience*. https://doi.org/10.1038/s41561-021-00729-w
645 Morrissey, A., & Scholz, C. A. (2014). Paleohydrology of Lake Turkana and its influence on the
646   Nile River system. *Palaeogeography, Palaeoclimatology, Palaeoecology*, *403*, 88-100.
647   https://www.sciencedirect.com/science/article/pii/S0031018214001552
648 Morrissey, A., Scholz, C. A., & Russell, J. M. (2018). Late Quaternary TEX86
649   paleotemperatures from the world's largest desert lake, Lake Turkana, Kenya. *Journal of
650   Paleolimnology*, *59*(1), 103-117. https://doi.org/10.1007/s10933-016-9939-6
651 Ng'ang'a, P., Muchane, M. W., Johnson, T. C., & Sturgeon, K. (1998). Comparisrison Of
652   Isotopic Records In Abiogenic And Biogenic Calcite From Lake Turkana, Kenya. In J. T.
653   Lehman (Ed.), *Environmental Change and Response in East African Lakes* (pp. 173-190).
654 Palacios-Fest, M. R., Cohen, A. S., & Anadón, P. (1994). Use of ostracodes as
655   paleoenvironmental tools in the interpretation of ancient lacustrine records. *Revista
656   Española De Paleontología*, *9*(2), 145-164.
657 Palacios-Fest, M. R., & Dettman, D. L. (2001). Temperature controls monthly variation in
658   ostracode valve Mg/Ca: Cypridopsis vidua from a small lake in Sonora, Mexico.
659   *Geochimica et Cosmochimica Acta*, *65*(15), 2499-2507.
660   https://www.sciencedirect.com/science/article/pii/S0016703701006020
661 Pérez, L., Curtis, J., Brenner, M., Hodell, D., Escobar, J., Lozano, S., & Schwalb, A. (2013).
662   Stable isotope values (δ¹⁸O & δ¹³C) of multiple ostracode species in a large Neotropical

663 lake as indicators of past changes in hydrology. *Quaternary Science Reviews*, *66*, 96-111.
664 https://doi.org/10.1016/j.quascirev.2012.10.044
665 Quinn, R. L., & Lepre, C. J. (2020). Revisiting the pedogenic carbonate isotopes and
666 paleoenvironmental interpretation of Kanapoi. *Journal of Human Evolution*, *140*, 102549.
667 https://doi.org/10.1016/j.jhevol.2018.11.005
668 Ricketts, R. D., & Anderson, R. F. (1998). A direct comparison between the historical record of
669 lake level and the δ^{18}O signal in carbonate sediments from Lake Turkana,
670 Kenya. *Limnology and Oceanography*.
671 https://aslopubs.onlinelibrary.wiley.com/doi/pdf/10.4319/lo.1998.43.5.0811
672 Ricketts, R. D., & Johnson, T. C. (1996). Climate change in the Turkana basin as deduced from a
673 4000 year long δO18 record. *Earth and Planetary Science Letters*, *142*(1-2), 7-17.
674 https://www.sciencedirect.com/science/article/pii/0012821X96000945
675 Roca, J. R., & Wansard, G. (1997). Temperature influence on development and calcification of
676 Herpetocypris brevicaudata Kaufmann, 1900 (Crustacea: Ostracoda) under experimental
677 conditions. *Hydrobiologia*, *347*(1-3), 91-95.
678 https://link.springer.com/article/10.1023/A:1003067218024
679 Schwalb, A., Burns, S. J., Cusminsky, G., Kelts, K., & Markgraf, V. (2002). Assemblage
680 diversity and isotopic signals of modern ostracodes and host waters from Patagonia,
681 Argentina. *Palaeogeography, Palaeoclimatology, Palaeoecology*, *187*(3-4), 323-339.
682 https://www.sciencedirect.com/science/article/pii/S0031018202004844
683 Talbot, M. R. (1990). A review of the palaeohydrological interpretation of carbon and oxygen
684 isotopic ratios in primary lacustrine carbonates. *Chemical Geology: Isotope Geoscience
685 section*, *80*(4), 261-279. https://doi.org/10.1016/0168-9622(90)90009-2
686 Thirumalai, K., Singh, A., Ramesh, R., & Ramesh, R. (2011). A MATLAB™ code to perform
687 weighted linear regression with (correlated or uncorrelated) errors in bivariate data. *Journal
688 of the Geological Society of India*, *77*(4), 377-380. https://doi.org/10.1007/s12594-011-
689 0044-1
690 Turpen, J. B., & Angell, R. W. (1971). Aspects of molting and calcification in the ostracod
691 Heterocypris. *The Biological Bulletin*, *140*(2), 331-338.
692 https://www.journals.uchicago.edu/doi/abs/10.2307/1540077
693 Uno, K. T., Polissar, P. J., Kahle, E., Feibel, C., Harmand, S., Roche, H., & deMenocal, P. B.
694 (2016). A Pleistocene palaeovegetation record from plant wax biomarkers from the
695 Nachukui Formation, West Turkana, Kenya. *Philosophical Transactions of the Royal
696 Society B: Biological Sciences*, *371*(1698), 20150235.
697 https://doi.org/10.1098/rstb.2015.0235
698 van der Lubbe, H. J. L., Krause-Nehring, J., Junginger, A., Garcin, Y., Joordens, J. C. A.,
699 Davies, G. R., Beck, C., Feibel, C. S., Johnson, T. C., & Vonhof, H. B. (2017). Gradual or
700 abrupt? Changes in water source of Lake Turkana (Kenya) during the African Humid
701 Period inferred from Sr isotope ratios. *Quaternary Science Reviews*, *174*, 1-12.
702 Von Grafenstein, U., Erlernkeuser, H., & Trimborn, P. (1999). Oxygen and carbon isotopes in
703 modern fresh-water ostracod valves: assessing vital offsets and autecological effects of
704 interest for palaeoclimate studies. *Palaeogeography, Palaeoclimatology, Palaeoecology*,
705 *148*(1-3), 133-152. https://www.sciencedirect.com/science/article/pii/S0031018298001801
706 Vonhof, H. B., Joordens, J. C. A., Noback, M. L., van der Lubbe, J. H. J. L., Feibel, C. S., &
707 Kroon, D. (2013). Environmental and climatic control on seasonal stable isotope variation
708 of freshwater molluscan bivalves in the Turkana Basin (Kenya). *Palaeogeography,*

709   *Palaeoclimatology, Palaeoecology*, *383-384*, 16-26.
710   https://doi.org/10.1016/j.palaeo.2013.04.022
711   Willmott, C. J., & Matsuura, K. (2001). Terrestrial Air Temperature and Precipitation: Monthly
712   and Annual Time Series (1950-1999) (Version 1.02). *Center for Climatic Research,*
713   *Department of Geography, University of Delaware.*
714   Wynn, J. G. (2004). Influence of Plio-Pleistocene aridification on human evolution: Evidence
715   from paleosols of the Turkana Basin, Kenya. *American Journal of Physical Anthropology*,
716   *123*(2), 106-118. https://doi.org/10.1002/ajpa.10317
717   Xia, J., Engstrom, D. R., & Ito, E. (1997). Geochemistry of ostracode calcite: Part 2. The effects
718   of water chemistry and seasonal temperature variation on Candona rawsoni. *Geochimica et*
719   *Cosmochimica Acta*, *61*(2), 383-391.
720   https://www.sciencedirect.com/science/article/pii/S0016703796003547
721   York, D., Evensen, N. M., Martínez, M. L., & De Basabe Delgado, J. (2004). Unified equations
722   for the slope, intercept, and standard errors of the best straight line. *American Journal of*
723   *Physics*, *72*(3), 367-369. https://doi.org/10.1119/1.1632486
724
725

726   **Figure Captions**

727

728   **Figure 1.** Regional (A) and local (B) setting of Lake Turkana, Kenya. (A) Mean annual
729   precipitation taken from the GPCC dataset (Beck et al. 2005). (B) Satellite imagery of Lake
730   Turkana with labelled sediment samples de- noted in yellow circles. Reference point (red circle)
731   is the marker from which proximity to Omo River inflow is computed.

732

733   **Figure 2. Temperature (A-B) and rainfall (C-D) climatology and interannual variability**
734   **over Lake Turkana and adjacent regions.** Mean annual values were computed as the average
735   of monthly temperatures over 1900-2017 from the University of Delaware dataset (Willmott &
736   Matsuura, 2001) and rainfall from the GPCC dataset (Beck et al. 2005). Interannual variability
737   was calculated as one standard deviation of annual-mean data from 1900-2017.

738

739   **Figure 3. Stable carbon and oxygen isotope analyses of ostracodes at Lake Turkana from**
740   **this study (blue) and previous studies (colors).** (A) $\delta^{18}O$ vs $\delta^{13}C$ (‰, VPDB) of various species
741   of ostracodes (differ- ent species indicated by shape) in Lake Turkana reported in previous work
742   and this study (blue circles). Note that measurements presented in this study are on individual
743   valves whereas the previous studies represent multi-specimen analyses. (B) $\delta^{18}O$ vs $\delta^{13}C$ of
744   specimens pooled by location in our study. Regression statistics reported in each subplot were
745   conducted using Maximum Likelihood Estimation using bivariate uncertainty (see Methods for
746   details).

747

748   **Figure 4. Average IOVA-$\delta^{13}C$ (A) and -$\delta^{18}O$ (B) in surface sediments from Lake Turkana**
749   **as a function of proximity to Omo River inflow.** Each data point represents the average of all
750   measurements on *S. clavularis* at each site and values are reported with respect to the VPDB
751   scale (‰). Distance from Omo River inflow was assigned based on a fixed reference point (see
752   Methods and Fig. 1 for details), and regression statistics were performed using Maximum
753   Likelihood Estimation. Errorbars represent combined root mean square errors of analytical
754   precision and intra-site isotopic variance.

755

756 **Figure 5. (A) Comparison of δ¹⁸Ow in Lake Turkana measured in 1994 versus those**
757 **reconstructed using individual ostracode valve analyses (IOVA) from samples collected in**
758 **1979 along with (B) annual rainfall anomaly between 1994 and 1979.** (A) δ¹⁸Ow
759 measurements (green circles) were taken from Ricketts and Johnson (1998) whereas IOVA-
760 based δ¹⁸Ow was reconstructed using IOVA-δ¹⁸O and *in situ* bottom-water temperature
761 measurements (Cohen, 1986) based on equilibrium isotope fractionation (see Methods for
762 details). Dashed lines depict linear regression lines of best fit (York et al. 2004) and errors
763 represent root mean square values of analytical precision and intra-site IOVA-δ¹⁸O variance. (B)
764 Rainfall anomaly of mean annual precipitation between 1993 and 1979 from the GPCC dataset
765 (Beck et al. 2005).

766 **Table 1.** Inter-site mean individual ostracode valve analyses (IOVA) of stable isotopes and valve characteristics (mass, length – L1,
767 width – L2) and *in situ* environmental parameters including pH, surface water and bottom water temperatures at site locations as well
768 as distance of site from a fixed marker in the Omo River inflow region (see Fig. 2). NA indicates not available.

Site #	Site ID	Lat (°N)	Lon (°E)	Depth (m)	Dist. (km)	pH	Sur. T (°C)	Bot. T (°C)	# IOVA	Avg. Mass (μg)	1σ Mass (μg)	Avg. L1 (μm)	1σ L1 (μm)	Avg. L2 (μm)	1σ L2 (μm)	Avg. δ¹³C (‰)	1σ δ¹³C (‰)	Avg. δ¹⁸O (‰)	1σ δ¹⁸O (‰)
1	BS125	4.3613	36.1988	1	50.0	9.1	NA	NA	13	166	39	2078	115	1074	219	-2.88	1.09	2.49	0.45
2	79-170F	4.2061	35.9535	14.5	65.0	9.1	27	26	22	249	36	2135	50	1124	33	-1.82	0.84	2.85	0.38
3	BS91	4.1369	36.2127	0.5	74.4	7.6	NA	NA	19	228	24	2085	71	1065	49	-2.21	1.23	3.15	0.43
4	BS90	4.1215	36.2179	0.2	76.4	10.3	NA	NA	15	218	48	2078	121	1030	143	-2.25	1.12	3.06	0.53
5	79-168F	4.0717	35.9230	15	80.6	9.1	27.5	23.5	21	230	42	2107	86	1105	53	-1.53	0.77	3.30	0.44
6	79-166F	3.9491	35.8664	10	94.8	9.1	29	27	15	194	37	2073	103	1087	31	-2.44	0.68	3.00	0.28
7	79-147F	3.7723	36.2214	9.5	114.3	9	25	24.7	21	156	57	1966	196	990	56	-1.22	1.10	3.40	0.53
8	79-164F	3.7386	35.8532	15.5	118.3	9.1	30	26.9	19	194	29	2055	79	1078	32	-1.49	1.19	3.25	0.31
9	79-130F	3.5659	35.9087	22	136.2	NA	27	26	21	228	33	2092	84	1106	51	-2.00	1.15	3.19	0.53
10	79-77F	3.5417	35.9589	29	138.4	8.7	NA	NA	20	237	26	2021	226	1150	214	-1.75	0.87	3.41	0.31
11	79-158F	3.4792	36.0490	27	145.0	9.1	NA	NA	21	277	35	2131	77	1117	47	-2.35	0.88	3.01	0.31
12	79-160F	3.4407	36.1774	37	150.0	NA	NA	NA	22	273	28	2137	66	1094	40	-0.95	0.83	3.62	0.38
13	79-183F	3.3115	36.0044	21	163.6	NA	NA	NA	20	238	45	2096	95	1095	49	-1.16	1.32	3.48	0.55
14	79-189F	3.0290	36.2264	31	195.7	NA	NA	NA	20	213	27	2036	76	1077	34	-1.80	1.12	3.55	0.32
15	79-204F	2.8216	36.6274	59	227.0	NA	NA	NA	23	220	49	2137	91	1127	63	-1.75	1.24	4.20	0.38
16	79-193F	2.7819	36.4219	59	226.0	NA	NA	NA	17	250	41	2107	127	1105	94	-1.51	0.79	3.96	0.57
17	79-194F	2.7380	36.5046	62	240.0	NA	NA	NA	18	222	43	2080	117	1108	80	-0.61	0.71	4.51	0.49
					Average	9.0	27.6	25.7	19.2	223	38	2083	105	1090	76	-1.75	1.00	3.38	0.42
					1σ	0.6	1.7	1.4	2.8	32	9	45	45	38	60	0.58	0.21	0.50	0.10

769

770 **Table 2.** Coefficient of determination (r^2) matrix between measured IOVA parameters pooled
771 across sites including valve characteristics (see Table 1 for abbreviations), $\delta^{18}O$, $\delta^{13}C$, and their
772 $1\sigma_{intra}$ variability with each other and with latitude, longitude, depth, and distance from Omo
773 River inflow. Note that correlations with pH and temperature measurements were not performed
774 due to incomplete datasets (Table 1). Asterisks (*) delineate r^2 values significant at the p<0.001
775 level.

	Avg. Mass	Avg. L1	Avg. L2	$\delta^{13}C$	$\delta^{13}C$ 1σ	$\delta^{18}O$	$\delta^{18}O$ 1σ
Distance	0.08	0.01	0.11	0.33*	0.00	0.81*	0.01
Latitude	0.09	0.01	0.12	0.32*	0.00	0.78*	0.01
Longitude	0.00	0.01	0.01	0.06	0.01	0.46*	0.11
Depth	0.16*	0.09	0.27*	0.32*	0.08	0.78*	0.00
Avg. Mass	x	x	x	x	x	x	x
Avg. L1	0.49*	x	x	x	x	x	x
Avg. L2	0.40*	0.32*	x	x	x	x	x
$\delta^{13}C$	0.04	0.00	0.00	x	x	x	x
$\delta^{13}C$ 1σ	0.08	0.03	0.12	0.02	x	x	x
$\delta^{18}O$	0.04	0.00	0.05	0.56*	0.01	x	x
$\delta^{18}O$ 1σ	0.01	0.00	0.13	0.07	0.05	0.04	x

776
777 **Table 3.** Investigation of oxygen isotope equilibrium of IOVA-$\delta^{18}O$ calcification. Comparisons
778 of measured versus calculated limnological parameters where $\delta^{18}O_w$ was computed using IOVA-
779 $\delta^{18}O$ averages and measured bottom water temperature in Eqn. (1), whereas bottom water
780 temperature was calculated using average IOVA-$\delta^{18}O$ and measured $\delta^{18}O_w$. Errors (reported as $\pm$
781 1σ) were propagated in the calculated values using a Monte Carlo procedure based on a root
782 mean square combination of sampling (*i.e.,* intra-site 1σ) and analytical uncertainty.

Domain	Avg. IOVA-$\delta^{18}O$ (‰, VPDB)	n	Measured $\delta^{18}O_w$ (‰, VSMOW)	n	Measured Bot. T (°C)	n	Calculated $\delta^{18}O_w$ (‰, VSMOW)	Calculated Bot. T (°C)
North of 3.9°N	2.98 ± 0.28	105	5.86 ± 0.56	19	25.3 ± 1.5	4	5.96 ± 0.3	25.3 ± 2.8
Koobi Fura Spit	3.11 ± 0.5	34	5.74 ± 0.57	17	23.5	1	5.73 ± 0.51	23.6 ± 3.2
All Samples	3.40 ± 0.62	329	5.72 ± 0.71	37	25.7 ± 1.4	6	6.4 ± 0.5	22.5 ± 3.8

783